ELSEVIER

Chemical Engineering Journal 139 (2008) 118–127

Chemical Engineering Journal

www.elsevier.com/locate/cej

Assessing dissolution kinetics of powders by a single particle approach

A. Marabi [a,b,*], G. Mayor [a], A. Burbidge [a,c], R. Wallach [d], I.S. Saguy [b]

[a] *Nestlé Research Center, Food Science Department, PO Box 44, CH-1000 Lausanne 26, Switzerland*
[b] *Institute of Biochemistry, Food Science and Nutrition, Faculty of Agricultural, Food and Environmental Quality Sciences, The Hebrew University of Jerusalem, PO Box 12, Rehovot 76100, Israel*
[c] *School of Engineering, University of Wales, Singleton Park, Swansea SA2 8PP, United Kingdom*
[d] *Department of Soil and Water Sciences, Faculty of Agricultural, Food and Environmental Quality Sciences, The Hebrew University of Jerusalem, PO Box 12, Rehovot 76100, Israel*

Received 2 May 2007; received in revised form 23 July 2007; accepted 24 July 2007

Abstract

A novel methodology for studying the dissolution of powders based on a "*single particle*" approach is presented. A single particle is the basic unit composing the bulk of a powder, and vast information could be gained from its dissolution kinetics. The dissolution of a single particle was measured by means of a microscopy-based experimental method with custom-developed image analysis algorithms. The effects of various liquids and their physical properties on the dissolution kinetics were studied. A mathematical model based on a shrinking sphere was utilized to describe the dissolution process. The rate constant was derived from the experimental data for each tested condition and correlated with the viscosity of the dissolving medium. A significant effect, mostly at low viscosity values was found. The derived values are in accordance with the diffusive behavior as predicted from the Einstein–Stokes equation. Isothermal calorimetry was used to measure the enthalpy of dissolution, and correlated with the rate constant derived from the single particle dissolution measurements. Faster dissolution rate corresponded with the lowest endothermic dissolution enthalpy. Consequently, it is proposed that the dissolution of particles is not simply a mass transfer limited process and it also includes heat transfer related mechanism(s) that should be further studied.

Keywords: Dissolution; Powder; Mathematical modeling; Single particle approach; Image analysis; Dissolution calorimetry

1. Introduction

Dissolution phenomena have been studied for more than a century, possibly starting with the classic work of Noyes and Whitney [1]. The dissolution kinetics of powders is of critical importance in many industrial and consumer applications, ranging from food and pharmaceutical products, to chemicals, fertilizers, paints, etc. In the food industry in particular, it is one of the relevant factors that defines product quality. At the consumer level, rapid, easy and complete dissolution and reconstitution of powders in water or other liquid media (e.g., milk) is essential for practical use. The advantages offered by powders, such as low packaging and transport costs, microbiological and chemical stability and convenience [2,3], has led to an increase in the number of products that reached the market. These include, among others, mixes for vending machines, cold and hot soluble products, infant formula, soups, etc.

A vast amount of research has been devoted towards the understanding of the dissolution kinetics of powders, mainly in the pharmaceutical and food industries. In the former, standard methods are often utilized, which include the measurement of dissolution kinetics by means of a USP (U.S. Pharmacopeia) dissolution apparatus [4,5]. The theories often utilized to model the dissolution process are based on Fick's laws of diffusion, the Noyes and Whitney equation [1], Hixson and Crowell cube-root law [6], etc. Pillay and Fassihi [7] presented a review of the fundamental dissolution theories. Other empirical models include those developed by Niebergall et al. [8], based on a square-root dependency on weight, and Higuchi and Hiestand [9], based on a power of two-thirds-root dependency on weight. The methods frequently utilized for quantifying the dissolution process include: particle size analysis, conductivity, spectrophotometry, rheological measurements, refractometry, ultrasonic reflectance, optical fiber sensors, gravimetric methods and NMR. In the

* Corresponding author at: Nestlé Research Center, Food Science Department, PO Box 44, CH-1000 Lausanne 26, Switzerland. Tel.: +41 21 785 8784; fax: +41 21 785 8554.
E-mail address: alejandro.marabi@rdls.nestle.com (A. Marabi).

1385-8947/$ – see front matter © 2007 Elsevier B.V. All rights reserved.
doi:10.1016/j.cej.2007.07.081

food industry, however, there are fewer publications addressing the dissolution process. Some examples include the dissolution of sucrose [10,11] and lactose [12–14] crystals, guar gum [15–17], alginate powders [18] and pectin [16,19]. Other fields that present well developed theories and experimental methods include metallurgical and chemical engineering. Some typical examples include the dissolution of alumina powder [20], alloys [21], sand [22] or virtual granules [23].

In the general case, the dissolution rate of a pure substance depends on the total resistance of three possible sequential stages of the process: diffusional supply of solvent to the dissolving surface, the transition of dissolved substance from solid to solute state immediately at the dissolution surface and the transport of solute (by diffusion and/or convection) from the surface to the bulk of solvent [24]. It is evident that in these processes the physical and chemical properties of the liquid medium (e.g., surface tension, viscosity, density, temperature) and those of the powder itself (e.g., particle size, density, porosity, chemical composition) affect the kinetics of the dissolution process.

The common approach for studying the dissolution kinetics of powders could be characterized as a "*bulk approach*" indicating that the dissolution process is studied by utilizing a considerable amount of powder, and as a consequence the phenomena occurring around each particle were not fully considered. The present work suggests a new methodology based on a "*single particle*" approach. A single particle is the basic unit composing the bulk of a powder, and vast information could be gained by understanding its dissolution kinetics. Moreover, the most important feature determining the bulk properties of a powder are the characteristics of the single particles it is composed of [25]. This knowledge could eventually be extended to the dissolution of a multiparticle assembly, by means of experimental work and/or mathematical modeling. It is worth noting that this approach was scarcely applied in the past, and only few papers analyzed different processes at this scale. As a consequence one could assume that the considerable amount of information that could be obtained concerning the kinetics of the dissolution process at the single particle level was not fully utilized. A brief summary of published works investigating mainly the dissolution of single particles (in chronological order) follows: Ready and Cooper [26] presented the differential equations governing the dissolution or growth of a sphere of finite initial radius controlled by mass diffusion. They included the effects of a moving boundary and the resulting radial convective transport. Vrentas and Shin [27,28] addressed the slow and fast growth or dissolution rates of isolated spheres, and developed a perturbation solution for the moving boundary problem. Dorozhkin [29] investigated the kinetics of phosphate rock dissolution utilizing images of single dissolving particles, and modeled the dissolution process by means of the Fokker–Plank equation. Bechtloff et al. [30] studied the dissolution of single borax crystals in propionic acid, but no mathematical description of the process kinetics was presented. Raghavan et al. [13] presented the dissolution kinetics of α-lactose monohydrate single crystals, and obtained linear dissolution profiles as a function of time for almost all the crystal faces investigated. Prokop'ev et al. [31] utilized a Monte Carlo simulation to study the development of surface roughness during dissolution of SiO_2 spherical particles, and concluded that the formation of roughness has an especially large effect on the dissolution of intermediate-size particles, for which the dissolution time has the same order of magnitude as the time required for establishment of the steady-state roughness. Bhandari and Roos [10] studied the dissolution of single sucrose crystals in molten sorbitol at different temperatures by means of microscopy. However, the kinetics of the process was not assessed. Štěpánek [23] modeled the dissolution of single granules according to the local fluxes obtained as the solution of a convection–diffusion equation, and determined the effective dissolution rate. The dissolution behavior as related to the granule structure was presented, based only on virtual dissolution experiments.

The thermodynamic aspects of the dissolution of powders can also be addressed by isothermal calorimetry. This is a widely utilized technique, mostly in the pharmaceutical field. More specifically, solution calorimetry is utilized for quantifying the heat of solution as a solid dissolves in a liquid. The theory behind the technique was previously explained in detail [32]. The number of applications of this technique is still growing. Examples from recent publications include its use to determine the wettability of finely divided solids [33,34], to differentiate (and/or quantify) between the amorphous and crystalline state of the same material [32,35–37], to monitor swelling and dissolution of polymers [38], etc.

In light of the literature data aforementioned, it is clear that a comprehensive study that includes both experimental work and mathematical modeling on the dissolution process and its dependence on various parameters is needed. Furthermore, the development of a mathematical model that incorporates the dissolving medium properties and particle characteristics, should eventually lead to a better understanding of the process of powders dissolution ultimately facilitating better prediction of its kinetics and fundamental understanding of the governing mechanisms.

The overall objectives of the present work were: (I) to develop an experimental method for quantifying the dissolution kinetics of single particles and to model the effects of the liquid properties on the dissolution kinetics and (II) to establish a relationship between the enthalpy of dissolution and the kinetics of the process.

2. Materials and methods

2.1. Model powder

Pure sucrose spherical particles (Freund Corp. Tokyo, Japan) were utilized in the present study as a model powder. These particles have two important advantages: (a) they are of homogeneous composition and (b) their spherical geometry is simple to deal with both experimentally and mathematically.

2.2. Physical characterization of the model powder

The particle apparent density, ρ_a, was determined with an AccuPyc 1330 (Micromeritics, Norcross, GA) utilizing He gas.

Samples were purged 10 times before the measurements. Ten replicates were automatically made for each sample, and the mean values are reported. The substance density, ρ_s, was measured as described above after grinding the samples. The bulk density, ρ_b, was measured with a GeoPyc 1360 (Micromeritics, Norcross, GA), utilizing a free-flowing dry powder (DryFlo) as the displaced medium. The total (ε_t), open (ε_o) and closed (ε_c) porosities were then calculated according to [39]

$$\varepsilon_t = 1 - \frac{\rho_b}{\rho_s} \quad (1)$$

$$\varepsilon_o = 1 - \frac{\rho_b}{\rho_a} \quad (2)$$

$$\varepsilon_c = \varepsilon_t - \varepsilon_o \quad (3)$$

The particle size distribution was characterized with a Mastersizer S and a small volume sample dispersion unit (Malvern Instruments, Malvern, UK). The particles were dispersed at ca. 1000 RPM in an organic medium composed by medium chain triglicerides (Delios V, Cognis, Illertisen, Germany). The polydisperse analysis model and the Fraunhofer configuration were utilized. The result are expressed by means of several statistics, including: $D[v, 0.1]$, $D[v, 0.5]$, $D[v, 0.9]$, $D[4, 3]$ which is the mean diameter based on the volume of the samples, and $D[3, 2]$ which is the mean diameter as based on the surface of the particles (usually denoted as the "Sauter diameter"). The cumulative percentage undersize curve was fitted with the Rosin–Rammler distribution function according to [40]

$$Y = 1 - \exp\left[-\left(\frac{x}{x_R}\right)^n\right] \quad (4)$$

where Y is the cumulative volume fraction under size x, x_R the constant giving a measure of the present particle size range and n is another constant characteristic of the analyzed material that gives a measure of the steepness of the cumulative curve. Lower values of n are associated with a more scattered distribution, while higher values of n imply an increasingly uniform particle structure.

2.3. Scanning electron microscopy (SEM)

The samples were observed with a SEM (Quanta 200F, FEI, Eindhoven) operating in environmental mode. Several magnifications were produced at different pressures (0.80–1.70 Torr).

2.4. Dissolution experiments

The image acquisition setup included an Axiovert 25 inverted microscope (Carl Zeiss, Feldbach, Switzerland) coupled to a USB camera (Scalar Corp., Tokyo, Japan). Transmitted (i.e., diascopic) light was utilized, as well as objective and optical enlargements of 35× and 1.5×, respectively. The movies were recorded at a framing frequency of 0.5 s^{-1}, in high-resolution mode (BTVPro software; http://www.bensoftware.com). For measuring the dissolution kinetics, single particles were carefully placed in the corresponding medium (0.1 ml) at 30.0 ± 1.0 °C in custom-made micro-cells. The image acquisition was started before the immersion of the particles. All the experiments were carried out at least in triplicate and mean values are reported. A series of liquids were utilized in the dissolution experiments, allowing for a wide and controlled range of physical properties. The liquids utilized were water (Milli-Q), ethylene glycol (EG), and polyethylene glycol (PEG) with average molecular weights of 200, 600 and 1000 (Sigma–Aldrich). All the liquids were utilized as received. The liquids were mixed with Millipore water in order to obtain final solutions with 10, 20, 30, 40, 50 and 60% (v/v) concentrations.

2.5. Image analysis

The recorded movies were analyzed with Object Image [41], a public domain image analysis program based on NIH software [42]. A custom-developed algorithm was utilized, which calculates the minimum, maximum and average particle diameter, as well as the diameter based on the surface area of the observed object in each frame. Basically, several operations are performed in each frame, such as thresholding, inversion, border recognition, etc. The numerical data obtained was then utilized for further analysis (e.g., data reduction, plotting).

2.6. Viscosity of the liquid solutions

The viscosity of the solutions was measured on a Modular Compact Rheometer (MCR500, Paar-Physica) with a bob and cup geometry. All the liquids were pre-equilibrated and the measurements were carried out at 30.0 ± 0.1 °C. A flow curve was generated by increasing the shear rate from 0.1 to 100 s^{-1} in a Ramp log mode. At least three replicates were made for each liquid and the mean values are reported.

2.7. Dissolution calorimetry

In order to quantify the heat of dissolution of the powder into the different mixtures utilized, measurements were carried out isothermally (30 ± 0.002 °C) in a Calvet calorimeter (Setaram C80, Caluire, France). In brief, the liquid (2 ml) and the powder (ca. 0.15 g) are placed separately in a special cell (reversal mixing), which is then introduced in the calorimeter and thermally equilibrated for at least 2 h. In preliminary studies, several amounts of the solid samples were tested in order to evaluate the influence of the liquid/solid ratio in the enthalpy values measured. It was found that the above quantities do not affect the results, as long as the solid is completely soluble in the amount of liquid utilized. The rotation of the apparatus is started after attaining equilibrium, bringing about the contact of the solid and liquid. The heat released or absorbed is measured in relation to a reference cell containing the same amount of water. A calorimetric curve is obtained and the data is treated for baseline corrections, and the area under the curve automatically integrated (SetSoft 2000 Software, Setaram) yielding the heat (J/g) adsorbed or released during the complete dissolution of the solid sample. All the measurements were repeated at least twice and average values are presented. The calorimeter was

calibrated both by dissolution of a standard material (KCl) and by means of the Joule effect. The heat of dissolution of the KCl was very similar to that in the reference literature [43,44], and the electrical calibration yielded a correction factor of 0.999. Consequently, there was no need to correct the experimental data obtained. A blank of water was also carried out, in order to verify the noise of the measurement, and to obtain a common baseline for all experiments.

2.8. Sucrose crystallinity

The degree of crystallinity in the solid sample was derived from the measurement of the heat of dissolution as stated above. The value obtained for the dissolution of the sample in pure water was converted into the percent of crystallinity by means of the relationship previously presented by Gao and Rytting [32]. Calorimetric measurements were also carried out using a Seiko 220C DSC (Tokyo, Japan) with a heating rate of 5 °C/min. The analyses were carried out with approximately 20 mg of sample hermetically sealed in an aluminum pan. An empty aluminum pan was used as a reference.

3. Mathematical modeling of the dissolution process

After evaluating various models, the shrinking sphere model [20] was chosen initially to fit the experimental data. This simple model describes the concentration of the dissolved solid as a function of time and is widely utilized in pharmaceutical and metallurgical domains. In this model, the rate of reaction is assumed to depend only on the surface area of the dissolving particle, which was regarded as a shrinking smooth sphere. Thus

$$R = kA \tag{5}$$

where R is the rate of dissolution (mg/s), k the rate constant (mg/(s cm^2)) and A is the surface area of the sphere (cm^2). The initial surface area of the spherical particle, A_0, is given by

$$A_0 = \frac{3M_0}{\rho_a r_0} \tag{6}$$

where M_0 is the initial mass (mg), ρ_a the particle apparent density (mg/cm^3) and r_0 is the particle initial diameter (cm). The surface area of the particle will decrease as the mass of the undissolved sphere decreases by the relationship:

$$A = A_0\left(\frac{M}{M_0}\right)^{2/3} \tag{7}$$

where M is the undissolved mass (mg) at time t (s). The undissolved sucrose mass can be related to the sucrose concentration in the liquid by

$$M - M_0 - (C - C_1)V \tag{8}$$

where C_1 is the initial sucrose concentration (mg/ml) in the liquid (and equals to zero for all the current experiments), C the sucrose concentration (mg/ml) at time t, and V is the liquid volume (ml). Combining Eqs. (5)–(8), an expression is then obtained for the rate of dissolution of sucrose:

$$R = \frac{dC}{dt}V = kA_0\left(1 - \frac{V}{M_0}C\right)^{2/3} \tag{9}$$

By rearranging this equation, integrating with respect to concentration and time, and introducing the initial condition $C(0) = 0$, the following expression is obtained:

$$C = \frac{M_0}{V}\left[1 + \left(\frac{A_0 k}{3M_0}t - 1\right)^3\right] \tag{10}$$

The mass transfer rate (k) was obtained by fitting Eq. (10) to the experimental data for the different test conditions. Mean values and standard deviation of at least three independent measurements are reported.

It is worth noting that the shrinking sphere model is used herein as a first approximation to describe the process' kinetics. A mathematical model based on the moving boundary theory (generally known as the "Stefan Problem"), that might better describe the dissolution process, is currently under development.

4. Results and discussions

The characteristic physical properties of the model powder are summarized in Table 1. The value of x_R, as derived from fitting the Rosin–Rammler distribution to the data ($R^2 > 0.99$; $P < 0.001$) is comparable to that of the $D[v, 0.5]$. Also, the derived value for n, is higher than 4.4, which was previously reported for commercial sugar [40], and indicates a relatively narrow particle size distribution.

Fig. 1 presents the particle size distribution of the fraction utilized in the dissolution experiments. Fig. 2 shows the microstructure of the particles, in which some surface roughness could be seen. The internal structure is clearly divided in two different areas: the internal core, which is a single sucrose crystal and the external surrounding area, which was added by a special granulation method. The samples were found to be 100% crystalline, by both the dissolution calorimetry and DSC methods (data not shown).

The receding boundaries of the particles during dissolution are presented in Fig. 3. These images, which provide a visual

Table 1
Physical properties of the samples evaluated in the dissolution experiments

Physical property	Mean values
Bulk density (g/cm^3)	1.253
Apparent density (g/cm^3)	1.533
Substance density (g/cm^3)	1.634
Open porosity (%)	18.3
Total porosity (%)	23.3
Closed porosity (%)	5.0
$D[v, 0.1]$ (μm)	397
$D[v, 0.5]$ (μm)	586
$D[v, 0.9]$ (μm)	706
$D[4, 3]$ (μm)	565
$D[3, 2]$ (μm)	530
x_R (μm)	613
n	5.6

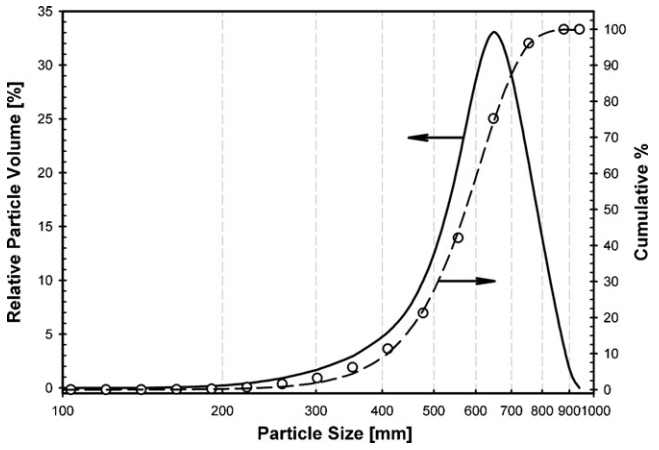

Fig. 1. Characterization of the particle size distribution for the spherical sucrose particles utilized in the dissolution experiments. The fitting of the Rosin–Rammler distribution function (dashed line) is shown for the cumulative function.

notion of the process, were utilized to derive the time dependence of the sample properties (e.g., min, max and mean diameter). The effect of the different solutions on the dissolution kinetics could be clearly seen, i.e., the complete dissolution of a particle in water takes ca. 70 s, while in a 50% PEG1000 solution ca. 1100 s.

It is worth noting that the particle is assumed to be spherical during the whole dissolution process. This assumption could be examined by deriving the aspect ratio of the measured particle at each time step [45]:

$$\text{aspect ratio} = \frac{\text{max dimension}}{\text{min dimension}} \tag{11}$$

The derived aspect ratio of the dissolving particles is very close to one for most of the dissolution process. Usually, the maximum deviation was around 5%, and below 10%. This supports the assumption that the particles remained spherical throughout the dissolution process.

The normalized diameter and dissolved mass of the particles were plotted against the dissolution time (Fig. 4a and b, respectively). The results are illustrated only for the case of dissolution in different PEG600 solutions (similar results were obtained for all the experiments). This behavior is typical of dissolving particles regardless of the method utilized for measuring the change in mass with time, and similar data have been reported for limestone particles [46], micronized drug powder [5], alumina [20],

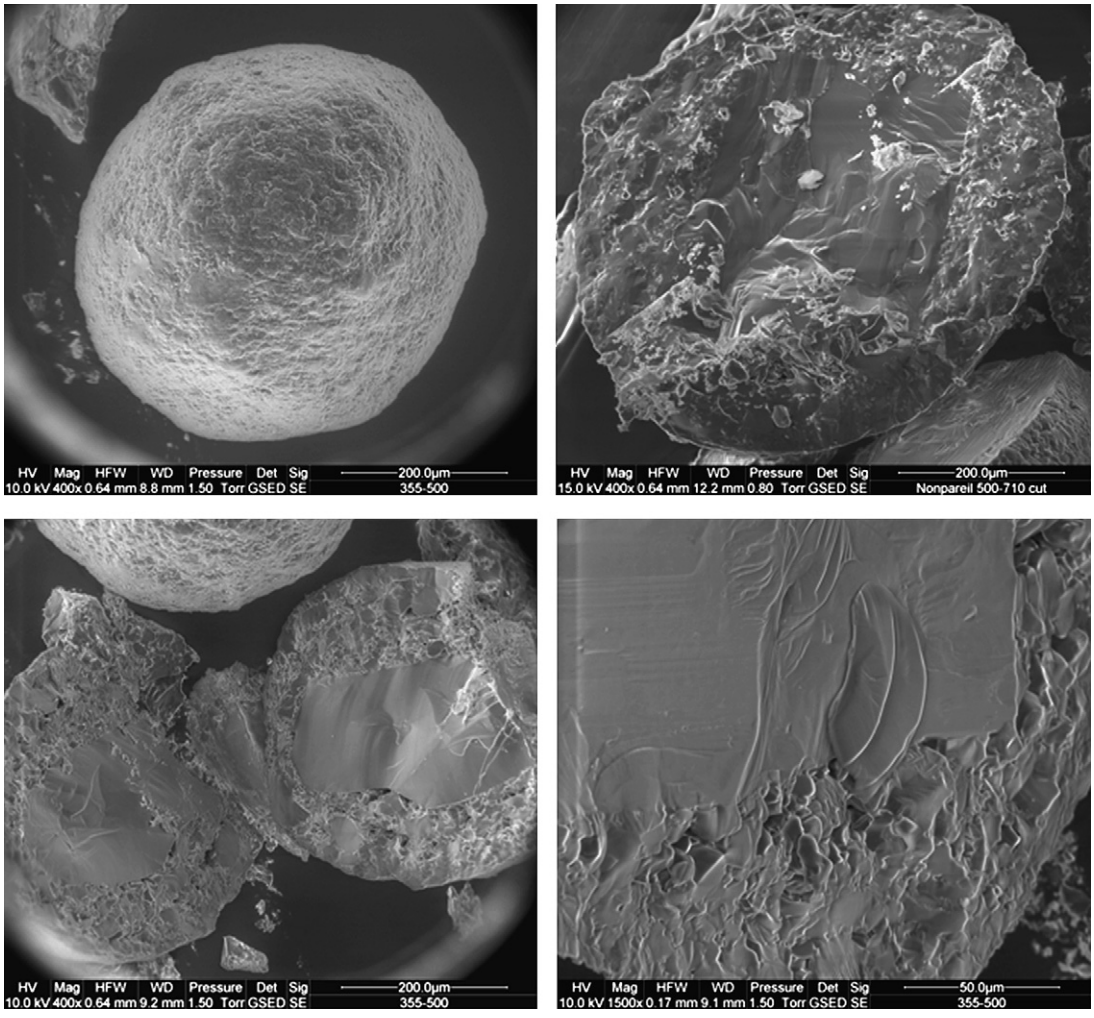

Fig. 2. SEM microphotographs of the spherical sucrose samples, showing the different internal and external structure.

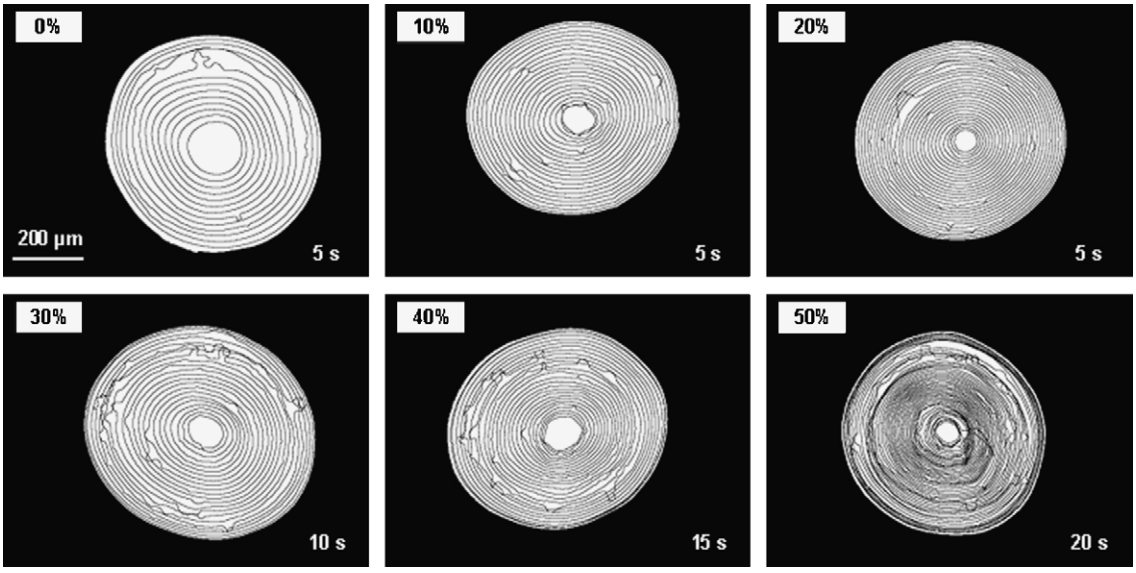

Fig. 3. Typical images for a dissolving sucrose sphere showing the moving boundaries as a function of time. The experiment was carried out at 30 °C with different concentrations of PEG1000 (denoted on each picture). The scale bar is the same for all conditions. Note the time scale between two consecutive lines as listed on the pictures.

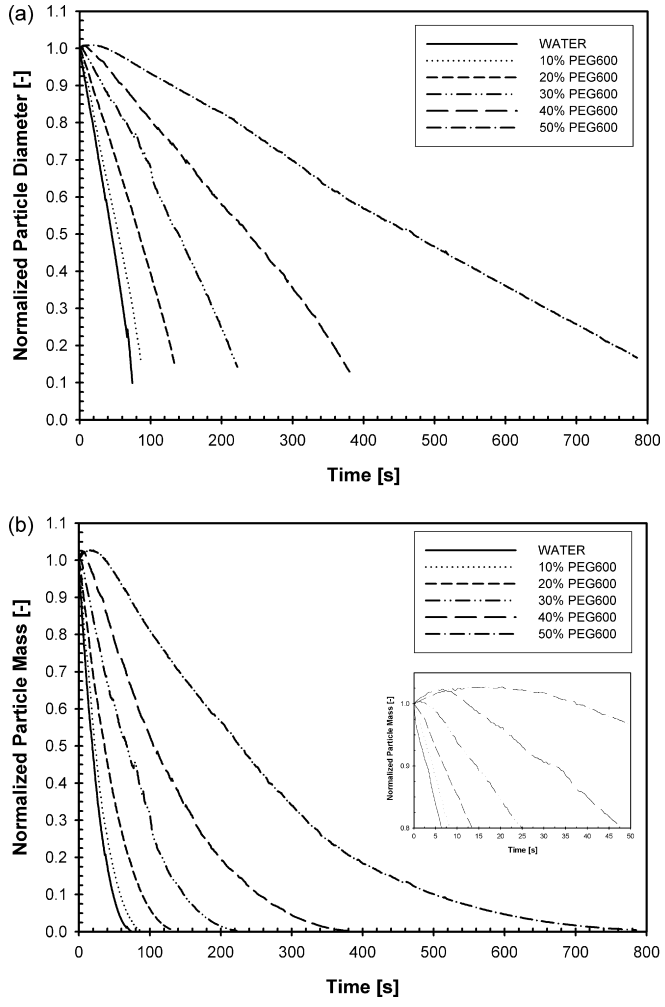

Fig. 4. Dissolution of spherical sucrose particles in PEG600–water mixtures: (a) normalized particle diameter and (b) normalized particle mass.

alginate powder [18] and sucrose crystals [11]. It is worth noting that all these data were derived from "multiparticle" experiments, whereas our results are derived from measurements on a single particle.

A change in the dissolution speed could be expected due to the presence of the two different zones in the sucrose particles. However, this was not observed, regardless of the liquid solution utilized. It could be that the dissolution speed is very similar in both zones, and/or the experimental method is unable to detect the minute differences if they exist. Preliminary experiments were made in which the image acquisition rate was increased (up to 10 frames/s), however, even under these conditions no differences were observed.

It is worth noting that swelling of the particles was observed during the first stages of the dissolution process with some of the liquids with high concentrations of PEG600 and PEG1000 (see inset in Fig. 4). This may be due to a faster rate of the liquid imbibition into the particle pores compared to the slower dissolution rate of the solid. The dissolution process starts following this imbibition period, and continues until the complete particles disappearance.

Typical fits of the shrinking sphere model (Eq. (10)) with the experimental data are depicted on Fig. 5, for mixtures of 10% (v/v) of the organic compounds in water. The fitted k value was derived by minimizing the sum of squares between the experimental data and those calculated by utilizing Eq. (10). It ranges from 0.643 ± 0.057 to 0.014 ± 0.005 mg/(s cm^2) for dissolution in water and 60% PEG600, respectively. The differences in the final concentration is a result of the different initial mass of each particles tested. However, and in contrast to other methods of assessing the dissolution kinetics of powders, these values are actually measured in each experiment and not derived from an overall set of particles with a more or less wide particles size distribution.

For all the mixtures tested, the k decreased with increasing concentration of the organic liquids. The slower dissolution

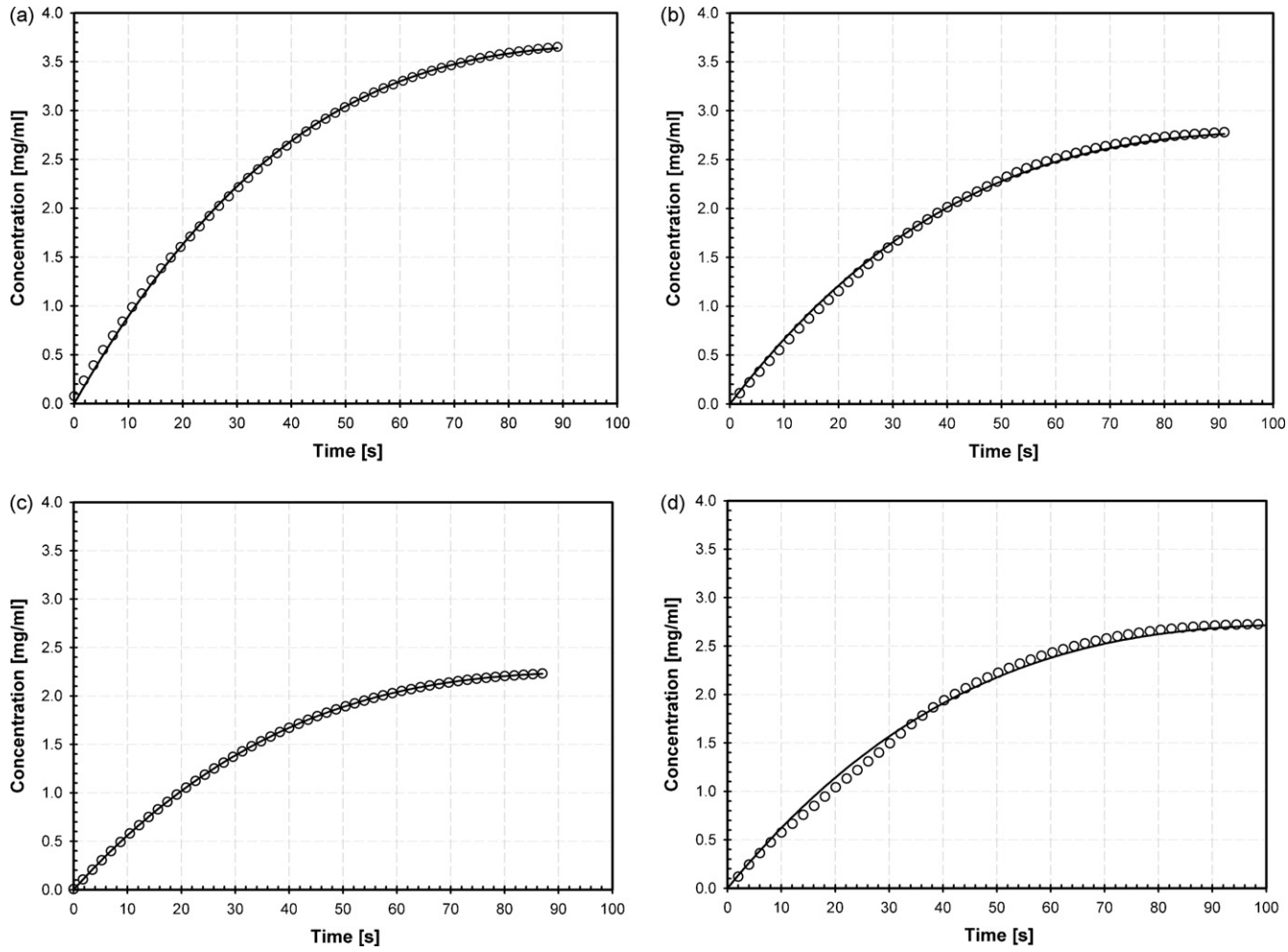

Fig. 5. Fitting of the shrinking sphere model to experimental data for 10% (v/v) mixtures. (a) EG, (b) PEG200, (c) PEG600 and (d) PEG1000.

rate in more concentrated solutions may be correlated with the increase of viscosity and indirectly affected by other properties such as the density, dielectric constant, or surface tension, which for extreme cases led to the above-mentioned swelling behavior of the particles.

Fig. 6 depicts the experimental data expressed as the normalized concentration in the liquid solutions. The time to complete dissolution ranges from ca. 65 to 220 s in water and 40% ethylene glycol mixture, respectively. A similar trend was observed for all other liquids tested.

Assuming that mass diffusion governs the dissolution process, it is possible to derive the effective diffusion coefficient (D_{eff}) from the Einstein–Stokes equation:

$$D_{\text{eff}} = \frac{K_{\text{B}}T}{6\pi a\mu} \tag{12}$$

where K_{B} is Boltzmann's constant (J/K), T the absolute temperature (K), a the hydrodynamic radius of the sucrose molecule (4.9×10^{-10} m) [47], and μ is the viscosity of the medium (Pa s). The effective diffusion coefficient was derived from the measured values of the viscosity for the different solutions. A plot of the rate constant as a function of the effective diffusivity resulted in a linear relationship as presented in Fig. 7a.

The data show that viscosity has a marked effect on the rate constant, particularly at low values. For example, when the viscosity was increased from 1.06 mPa s (for water) to only ca. 2.5 mPa s, the value of k decreased from 0.64 to ca. 0.25 mg/(s cm^2), and the time to complete dissolution increased

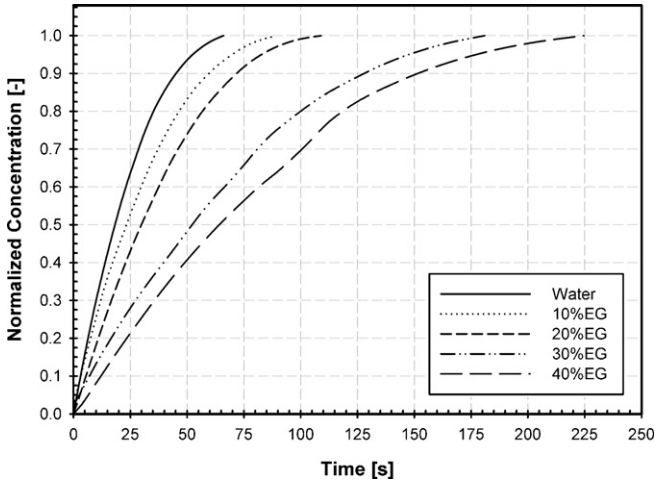

Fig. 6. Experimental data for the dissolution of spherical sucrose particles in different ethylene glycol–water mixtures.

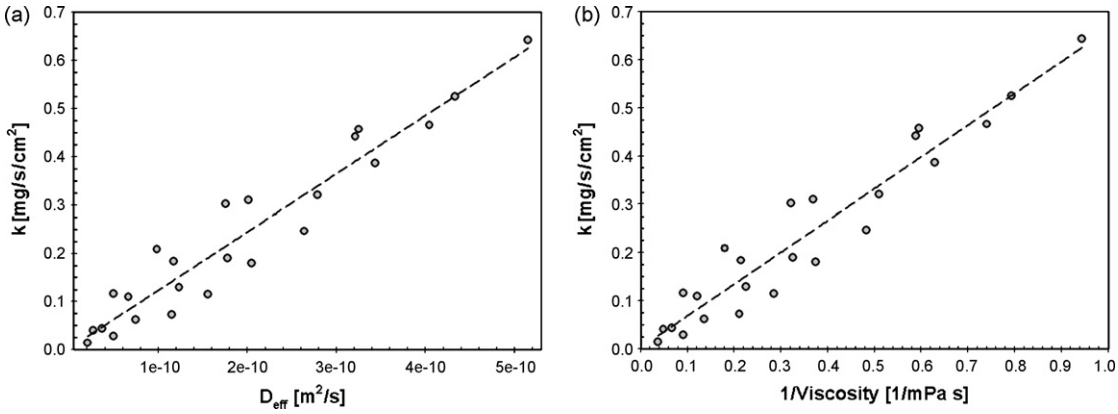

Fig. 7. (a) Correlation between the derived rate constant (k) and the effective diffusion coefficient as derived from Eq. (12). (b) Reciprocal correlation between the derived rate constant (k) and the viscosity of the dissolving medium.

from ca. 70 to 300 s, respectively. This effect has significant implications, since such low viscosity values are not uncommon in food formulations in which particulates should dissolve as fast as possible. In contrast, for values higher than 5 mPa s the change in the rate constant is not as pronounced; although all of the tested conditions led to very slow dissolution kinetics, with values of k always lower than 0.1 mg/(s cm^2).

Moreover, a linear correlation was found between the derived rate constant and the reciprocal of the viscosity (Fig. 7b), confirming the expected results according to the Einstein–Stokes equation. This suggests that the reaction rate constant, k, is effectively dominated by the diffusion process (characterized by D_{eff}) rather than the solubilisation rate at the particle surface for the current experimental conditions.

Other factors such as the density, surface tension and dielectric constant of the dissolving media were also found to affect the dissolution rate of the particles and they might have an indirect effect on the kinetics of the dissolution process. However, some of them have a more pronounced effect than others. Current efforts are directed towards the incorporation of the relevant parameters in an integrated model, allowing for accurate prediction of the dissolution kinetics as a function of the process parameters.

Basically, the dissolution enthalpy is a composite of wetting of the solid phase, liquid penetration, dissolution phenomena (including disruption of the solid lattice, removal of the surface molecules, disruption of the solvent and incorporation of the solute molecules in cavities in the solvent), dilution (the transfer of a molecule from the saturated solution to an infinitely dilute solution), possibly rearrangement and conformational changes [32,48–50].

The heat of dissolution in water measured for the spherical sucrose particles was 17.61 J/g (endothermic effect). Gao and Rytting [32] reported a similar value of 17.72 J/g. According to the measured value, and utilizing the relationship between the heat of solution and weight percent of crystalline sucrose [32] it is possible to conclude that the sample was 100% in a crystalline form. Moreover, from the DSC curves, no indication of a glass transition event was observed (data not shown). The degree of crystallinity or amorphous content of the sample is extremely important, since it is well known that endothermic values are measured for the former, whereas the enthalpy of dissolution reverts to exothermic values for the latter [32,36].

Fig. 8 shows the effect of increasing the amount of ethylene glycol in the calorimetric curves measured. Similar effects were found for all the other tested liquids. The dissolution process was found to be endothermic for all tested conditions. In general, the amount of absorbed heat increased with an increase in the concentration of the organic phase, ranging from 17.61 in water to ca. 45 J/g for the 60% solutions.

When the calorimetric curves for different liquids at the same concentration are compared, it could be observed that the endothermic response is comparable, independently of the solution utilized. A summary of the measured enthalpies for all the conditions tested is depicted in Fig. 9.

When all the derived rate constant values are plotted as a function of the measured enthalpy of dissolution, a negative linear correlation was obtained (Fig. 10). The highest value for the rate constant was observed for the case in which the dissolution medium was pure water, and corresponded to the lowest endothermic dissolution enthalpy measured. The slowest dissolution rates measured in the more concentrated solution corresponded to the higher endothermic enthalpies.

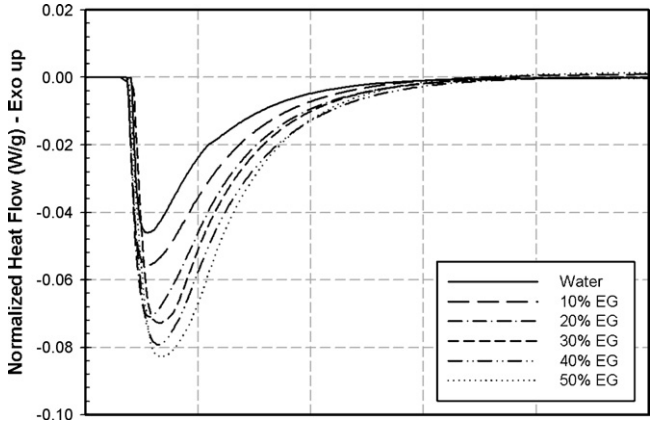

Fig. 8. Typical calorimetric curves for the dissolution of spherical sucrose particles in water and in mixtures of water and ethylene glycol.

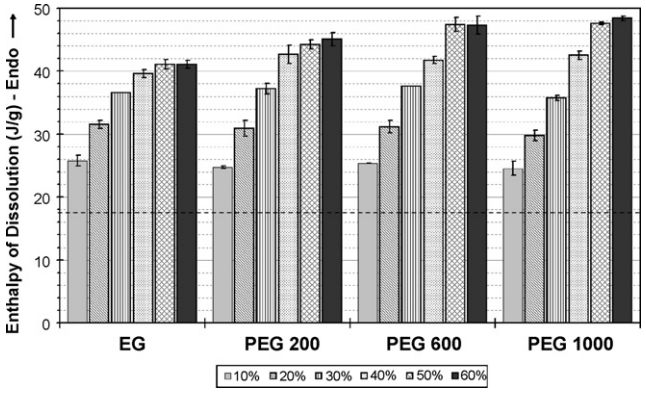

Fig. 9. Measured enthalpy of dissolution for the dissolution of sucrose spheres in the different solutions utilized. The dashed line indicates the enthalpy of dissolution in pure water.

Similar results were reported, yet, only the logarithms of the initial dissolution rate of the studied drugs were correlated with the enthalpies of the dissolution [51]. The authors explained the observed correlation between the dissolution rate and the enthalpy of the process on the basis of Gibbs free energy and the Noyes–Whitney equation [1].

The enthalpy of dissolution of amorphous sucrose (−47.7 J/g) was previously reported [36]. We have tried to quantify the dissolution kinetics of single amorphous sucrose particles, but the process was instantaneous and therefore impossible to measure with the current experimental setup. This indicates that the correlation found could be extended beyond the crystalline state of the material by utilizing fast video acquisition techniques; however, its linearity should be corroborated. On the other hand, limiting values of the enthalpy might exist for which the dissolution rate would be zero. These values could be obtained by extrapolating the regression line. In fact, negligible dissolution was observed when the fraction of the organic phase was higher than 70%. This correlation also suggests that the dissolution process might also be influenced by a heat transfer mechanism and not only governed by mass transfer. The high correlation factor obtained ($R^2 = 0.96$; $P < 0.0001$) is also an indication of the agreement between the process kinetics measured at the single particle level with the thermodynamic results obtained from a well-based methodology as calorimetry. Further work is under way in order to better understand the observed effects with more complex systems.

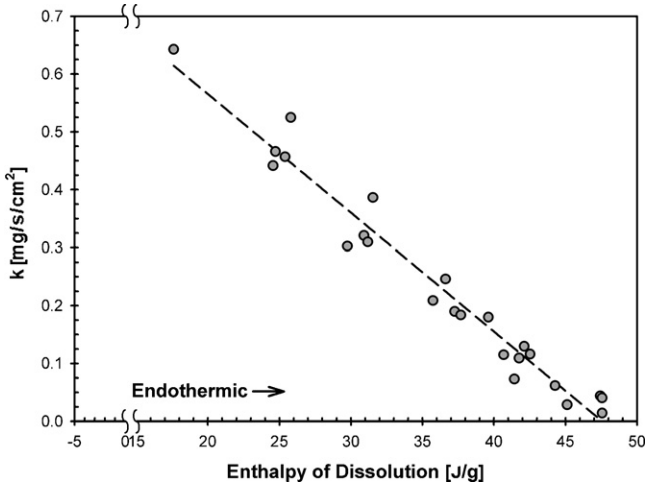

Fig. 10. Correlation between the enthalpy of dissolution and the rate constant (k) for sucrose spheres dissolved in different the solutions.

5. Conclusions

A microscopy-based experimental method and appropriate image analysis algorithms were developed for measuring the dissolution of a single particle. The effects of various liquids and their physical properties on the dissolution kinetics were quantified. A mathematical model based on a shrinking sphere was utilized to describe the dissolution process. The particles' diameter decreased linearly with time during the dissolution process while the spherical shape was retained throughout. For high concentrations of the organic liquids tested, a short swelling period was observed at the beginning of the process, after which the particles eventually started to dissolve. A rate constant was derived for each tested condition by fitting the shrinking sphere model to the experimental data. The effect of liquid viscosity on the dissolution kinetics of a single particle was correlated with this rate constant and a significant effect, mostly at low viscosity values, was found. The derived values of the effective diffusion of sucrose are in accordance with the diffusive behavior as predicted from the Einstein–Stokes equation. Isothermal calorimetry was used to measure the enthalpy of dissolution, and correlated with the rate constant derived from the single particle dissolution measurements. Faster dissolution rate was observed in pure water, corresponding to the lowest endothermic dissolution enthalpy whereas slower dissolution rates corresponded to higher endothermic enthalpies. It is proposed that the dissolution process might not be solely a mass transfer limited process; heat transfer processes could also have a significant effect on the overall rate. Additional research to further elucidate the mechanism(s) involved in single particle dissolution is required.

References

[1] A. Noyes, W.R. Whitney, The rate of solution of solid substances in their own solutions, J. Am. Chem. Soc. 19 (1897) 930–934.
[2] M.F. Edwards, T. Instone, Particulate products—their manufacture and use, Powder Technol. 119 (2001) 9–13.
[3] P.J. Lillford, P.J. Fryer, Food particles and the problems of hydration, Chem. Eng. Res. Design 76 (1998) 797–802.
[4] J.T. Carstensen, M. Dali, Determination of mass transfer dissolution rate constants from critical time of dissolution of a powder sample, Pharm. Dev. Technol. 4 (1999) 1–8.
[5] S.N. Bhattachar, J.A. Wesley, A. Fioritto, P.J. Martin, S.R. Babu, Dissolution testing of a poorly soluble compound using the flow-through cell dissolution apparatus, Int. J. Pharm. 236 (2002) 135–143.
[6] A.W. Hixson, J.H. Crowell, Dependence of reaction velocity upon surface and agitation, Ind. Eng. Chem. 23 (1931) 923–931.
[7] V. Pillay, R. Fassihi, Unconventional dissolution methodologies, J. Pharm. Sci. 88 (1999) 843–851.
[8] P.J. Niebergall, G. Milosovich, J.E. Goyan, Dissolution rate studies. II. Dissolution of particles under conditions of rapid agitation, J. Pharm. Sci. 52 (1963) 236–241.

[9] W.I. Higuchi, E.N. Hiestand, Dissolution rates of finely divided drug powders. I. Effect of a distribution of particle size in a diffusion-controlled process, J. Pharm. Sci. 52 (1963) 67–71.
[10] B.R. Bhandari, Y.H. Roos, Dissolution of sucrose crystals in the anhydrous sorbitol melt, Carbohydr. Res. 338 (2003) 361–367.
[11] T. Koiranen, T. Kilpio, J. Nurmi, H.V. Norden, The modelling and simulation of dissolution of sucrose crystals, J. Cryst. Growth 199 (1999) 749–753.
[12] G.E. Hodges, E.K. Lowe, A.H.J. Paterson, A mathematical-model for lactose dissolution, Chem. Eng. J. Biochem. Eng. J. 53 (1993) B25–B33.
[13] S.L. Raghavan, R.I. Ristic, D.B. Sheen, J.N. Sherwood, Dissolution kinetics of single crystals of alpha-lactose monohydrate, J. Pharm. Sci. 91 (2002) 2166–2174.
[14] E.K. Lowe, A.H.J. Paterson, A mathematical model for lactose dissolution. Part II. Dissolution below the alpha lactose solubility limit, J. Food Eng. 38 (1998) 15–25.
[15] Q. Wang, P.R. Ellis, S.B. Ross-Murphy, Dissolution kinetics of guar gum powders. I. Methods for commercial polydisperse samples, Carbohydr. Polym. 49 (2002) 131–137.
[16] A. Parker, F. Vigouroux, W.F. Reed, Dissolution kinetics of polymer powders, AIChE J. 46 (2000) 1290–1299.
[17] Q. Wang, P.R. Ellis, S.B. Ross-Murphy, Dissolution kinetics of guar gum powders. II. Effects of concentration and molecular weight, Carbohydr. Polym. 53 (2003) 75–83.
[18] C.K. Larsen, O. Gaserod, O. Smidsrod, A novel method for measuring hydration and dissolution kinetics of alginate powders, Carbohydr. Polym. 51 (2003) 125–134.
[19] T.P. Kravtchenko, J. Renoir, A. Parker, G. Brigand, A novel method for determining the dissolution kinetics of hydrocolloid powders, Food Hydrocolloids 13 (1999) 219–225.
[20] R.G. Haverkamp, B.J. Welch, Modelling the dissolution of alumina powder in cryolite, Chem. Eng. Proc. 37 (1998) 177–187.
[21] F.J. Vermolen, P. van Mourik, S. van der Zwaag, Analytical approach to particle dissolution in a finite medium, Mater. Sci. Technol. 13 (1997) 308–312.
[22] A. Mgaidi, F. Jendoubi, D. Oulahna, M. El Maaoui, J.A. Dodds, Kinetics of the dissolution of sand into alkaline solutions: application of a modified shrinking core model, Hydrometallurgy 71 (2004) 435–446.
[23] F. Štěpánek, Computer-aided product design—granule dissolution, Chem. Eng. Res. Des. 82 (2004) 1458–1466.
[24] V.F. Frolov, Dissolution of disperse materials, Theor. Found. Chem. Eng. 32 (1998) 357–368.
[25] M.M. de Villiers, Influence of agglomeration of cohesive particles on the dissolution behaviour of furosemide powder, Int. J. Pharm. 136 (1996) 175–179.
[26] D.W. Readey, A.R. Cooper, Molecular diffusion with a moving boundary and spherical symmetry, Chem. Eng. Sci. 21 (1966) 917–922.
[27] J.S. Vrentas, D. Shin, Perturbation solutions of spherical moving boundary problems. II, Chem. Eng. Sci. 35 (1980) 1697–1705.
[28] J.S. Vrentas, D. Shin, Perturbation solutions of spherical moving boundary problems. I, Chem. Eng. Sci. 35 (1980) 1687–1696.
[29] S.V. Dorozhkin, Fundamentals of the wet-process phosphoric acid production. 1. Kinetics and mechanism of the phosphate rock dissolution, Ind. Eng. Chem. Res. 35 (1996) 4328–4335.
[30] N. Bechtloff, P. Jüsten, J. Ulrich, The kinetics of heterogeneous solid–liquid reaction crystallizations—an overview and examples, Chem. Ing. Tech. 73 (2001) 453–460.
[31] S.I. Prokop'ev, A.G. Okunev, Y.I. Aristov, A Monte Carlo simulation of the development of surface roughness and its effect on the dissolution kinetics, Colloid J. 64 (2002) 95–100.
[32] D. Gao, J.H. Rytting, Use of solution calorimetry to determine the extent of crystallinity of drugs and excipients, Int. J. Pharm. 151 (2006) 183–192.
[33] M. Lazghab, K. Saleh, I. Pezron, P. Guigon, L. Komunjer, Wettability assessment of finely divided solids, Powder Technol. 157 (2005) 79–91.
[34] D.A. Spagnolo, Y. Maham, K.T. Chuang, Calculation of contact angle for hydrophobic powders using heat of immersion data, J. Phys. Chem. 100 (1996) 6626–6630.
[35] D.P. Miller, J.J. de Pablo, H. Corti, Thermophysical properties of trehalose and its concentrated aqueous solutions, Pharm. Res. 14 (1997) 578–590.
[36] D.P. Miller, J.J. de Pablo, Calorimetric solution properties of simple saccharides and their significance for the stabilization of biological structure and function, J. Phys. Chem. B 104 (2000) 8876–8883.
[37] S.E. Dilworth, G. Buckton, S. Gaisford, R. Ramos, Approaches to determine the enthalpy of crystallisation, and amorphous content, of lactose from isothermal calorimetric data, Int. J. Pharm. 284 (2004) 83–94.
[38] S. Conti, S. Gaisford, G. Buckton, U. Cooke, Solution calorimetry to monitor swelling and dissolution of polymers and polymer blends, Thermochim. Acta 450 (2006) 56–60.
[39] H. Schubert, Food particle technology. I. Properties of particles and particulate food systems, J. Food Eng. 6 (1987) 1–32.
[40] H. Yan, G.V. Barbosa-Canovas, Size characterization of selected food powders by five particle size distribution functions, Food Sci. Technol. Int. 3 (1997) 361–369.
[41] N. Vischer, Object Image [2.09], 2002, http://simon.bio.uva.nl/object-image.html.
[42] W. Rasband, NIH Image [1.62], 2001, http://rsb.info.nih.gov/nih-image/.
[43] I. Wadsö, R.N. Goldberg, Standards in isothermal microcalorimetry (IUPAC technical report), Pure Appl. Chem. 73 (2001) 1625–1639.
[44] R. Ramos, S. Gaisford, G. Buckton, P.G. Royall, B.T.S. Yff, M.A.A. O'Neill, A comparison of chemical reference materials for solution calorimeters, Int. J. Pharm. 299 (2005) 73–83.
[45] J.C. Russ, Image Analysis of Food Microstructure, CRC Press, Boca Raton, 2005.
[46] T. Allers, M. Luckas, K.G. Schmidt, Modeling and measurement of the dissolution rate of solid particles in aqueous suspensions. Part II. Experimental results and validation, Chem. Eng. Technol. 26 (2003) 1225–1229.
[47] M. Mathlouthi, P. Reiser, Sucrose—Properties and Applications, Blackie Academic & Professional, London, 1995.
[48] G. Buckton, Applications of isothermal microcalorimetry in the pharmaceutical sciences, Thermochim. Acta 248 (1995) 117–129.
[49] G. Castronuovo, V. Elia, M. Niccoli, F. Velleca, Simultaneous determination of solubility, dissolution and dilution enthalpies of a substance from a single calorimetric experiment, Thermochim. Acta 320 (1998) 13–22.
[50] H. Piekarski, Applications of calorimetric methods to investigations of interactions in solutions, Pure Appl. Chem. 71 (1999) 1275–1283.
[51] K. Terada, H. Kitano, Y. Yoshihashi, E. Yonemochi, Quantitative correlation between initial dissolution rate and heat of solution of drug, Pharm. Res. 17 (2000) 920–924.